THE JOURNAL OF BIOLOGICAL CHEMISTRY VOL. 284, NO. 40, pp. 27377–27383, October 2, 2009

Myosin II Recruitment during Cytokinesis Independent of Centralspindlin-mediated Phosphorylation*[S]

Received for publication, June 1, 2009, and in revised form, July 29, 2009 Published, JBC Papers in Press, August 6, 2009, DOI 10.1074/jbc.M109.028316

Jordan R. Beach[‡§1] **and Thomas T. Egelhoff**[‡§2]

From the [‡]*Department of Cell Biology, Lerner Research Institute, Cleveland Clinic, Cleveland, Ohio 44195 and the* [§]*Department of Physiology and Biophysics, Case Western Reserve University School of Medicine, Cleveland, Ohio 44106*

During cell division, the mechanisms by which myosin II is recruited to the contractile ring are not fully understood. Much recent work has focused on a model in which spatially restricted *de novo* filament assembly occurs at the cell equator via localized myosin II regulatory light chain (RLC) phosphorylation, stimulated by the RhoA-activating centralspindlin complex. Here, we show that a recombinant myosin IIA protein that assembles constitutively and is incapable of binding RLC still displays strong localization to the furrow in mammalian cells. Furthermore, this RLC-deficient myosin II efficiently drives cytokinesis, demonstrating that centralspindlin-based RLC phosphorylation is not necessary for myosin II localization during furrowing. Myosin II truncation analysis further reveals two distinct myosin II tail properties that contribute to furrow localization: a central tail domain mediating cortical furrow binding to heterologous binding partners and a carboxyl-terminal region mediating co-assembly with existing furrow myosin IIA or IIB filaments.

Non-muscle myosin II, through its interaction with F-actin, is believed to be the dominant force-producing machinery utilized to separate daughter cells during cell division. Following anaphase onset, myosin II is recruited to the equatorial cortex where it assembles into the contractile ring. Despite much recent progress, the exact mechanism by which myosin II is recruited to and retained in the contractile ring in the proper spatio-temporal manner remains unclear.

Myosin II is a member of the myosin superfamily that binds F-actin and hydrolyzes ATP to produce force. A monomer consists of two myosin heavy chains ("MHCs"),[3] two essential light chains ("ELCs"), and two regulatory light chains ("RLCs") (see Fig. 1*A*). The MHC consists of an amino-terminal globular head domain often referred to as the "motor" domain. It is responsible for F-actin binding and ATP binding and hydrolysis. One RLC and one ELC associate with each MHC via two IQ motifs on a neck region linking the head and tail domain. The remainder of the MHC forms a continuous α-helix that interacts with another MHC rod to create a coiled-coil-mediated dimer. At the extreme C terminus, mammalian non-muscle myosin II molecules contain an ~30 residue "non-helical tailpiece." Many phosphorylation sites have been identified on both the RLC and the MHC (1–4). The best characterized of these sites is Thr-18/Ser-19 on the RLC, which, when phosphorylated, has been shown to activate myosin II by increasing the affinity of MHC for F-actin, consequently increasing the ATPase activity (5, 6). Phosphorylation of these sites is also able to convert myosin II from a folded 10 S "inactive" monomer into the extended 6 S monomer that readily forms filaments (7).

Mammalian genomes contain three genes encoding non-muscle myosin II heavy chain isoforms, *mhc IIA*, *IIB*, and *IIC*. MHC IIA and IIB are widely expressed in many tissues and cell lines, whereas IIC is expressed with a more limited distribution (8). In mice, gene knockouts of *mhc IIA* and *IIB* result in differing phenotypes that are only partially rescued by the other isoform, suggesting that both isoform-specific and overlapping roles exist (9). Previous reports have suggested that myosin IIA and IIB isoforms are capable of co-assembling into mixed or heterotypic filaments (10, 11). However, there is also evidence showing that myosin II isoforms have different subcellular localization in non-mitotic cells, supportinga model in which homotypic filaments are the dominant filamentous structure in live cells (12, 13). Whether myosin IIA and IIB can co-assemble in the contractile ring of dividing cells is not known.

The dominant model for furrow localization of myosin II during cell division hypothesizes spatially restricted equatorial activation and filament assembly via phosphorylation of the RLC on Thr-18/Ser-19. The most prominent upstream signaling pathway implicated in this furrow recruitment model is the centralspindlin pathway. In this pathway, the kinesin-6 protein MKLP1 anchors MgcRacGAP and a RhoGEF (ECT2) to the spindle midzone (14). This in turn locally activates RhoA, leading to activation of Rho kinase and/or citron kinase, both of which have been shown capable of phosphorylating RLC (15–18). Centralspindlin-based signals clearly contribute to myosin II-cytokinesis functions. However, whether these signals contribute to initial myosin II binding/recruitment, to myosin II contractile activation, or to both, is unresolved.

Another recent study reported that GFP-tagged RLC constructs with alanine substitutions at the activating Thr-18/Ser-19 sites were still able to localize to the furrow of dividing

* This work was supported, in whole or in part, by National Institutes of Health Grant GM 077224 (to T. T. E.).

[S] The on-line version of this article (available at http://www.jbc.org) contains supplemental Figs. S1 and S2.

[1] Supported by National Institutes of Health Training Grant DK07678.

[2] To whom correspondence should be addressed: Dept. of Cell Biology, NC10, Lerner Research Institute, Cleveland Clinic, 9500 Euclid Ave., Cleveland, OH 44195. Tel.: 216-445-9912; Fax: 216-444-9404; E-mail: Egelhot@ccf.org.

[3] The abbreviations used are: MHC, myosin heavy chain; NMHC, non-muscle MHC; ELC, essential light chain; RLC, regulatory light chain; GAP, GTPase-activating protein; GEF, guanine nucleotide exchange factor; ACD, assembly-competent domain; GFP, green fluorescent protein; EGFP, enhanced GFP; DAPI, 4′,6-diamidino-2-phenylindole; PBS, phosphate-buffered saline; siRNA, small interfering RNA.

HeLa cells, suggesting that RLC phosphorylation is not required for myosin equatorial localization (19). However, in that study, it was not clear how much endogenous wild type RLC was present; thus this result may represent a tracer amount of the T18A/S19A mutant RLC passively co-assembling with a larger pool of endogenous RLC-phosphorylated myosin II.

Another proposed model for myosin recruitment to the equatorial region of a dividing cell is cortical flow. In this model, supported by observations in both *Dictyostelium* and mammalian cells, myosin filaments move along the cortex and into the furrow in a motor-dependent manner (20–22). However, recent studies using total internal reflection fluorescence imaging in normal rat kidney cells revealed no detectable myosin II cortical flow (23), raising uncertainty as to whether cortical flow is an important mechanism for myosin recruitment in mammalian cells.

In this study, we provide the first evidence that mammalian myosin II can localize to the furrow of dividing cells independent of the regulatory light chain. These studies demonstrate that both robust myosin II recruitment to the furrow and efficient cell division can be achieved without spatially localized centralspindlin-mediated RLC phosphorylation. We conclude that other mechanisms such as cortical flow (22, 24) and/or equatorial myosin II binding partners (25, 26) must be sufficient for myosin II recruitment and cell furrowing in mammalian cells. Furthermore, we show that a headless myosin construct can localize to the contractile ring, supporting a model in which actin binding and ATPase activity are not required for myosin II recruitment. We also provide novel evidence that MHC isoforms are capable of co-assembling in the contractile ring.

EXPERIMENTAL PROCEDURES

DNA Mutagenesis—Amino acid numbering is based on GenBank™ accession number NM_002473. The plasmids pEGFP-C3-NMHC-IIA, pCMV-EGFP-NMHC-IIAΔIQ2, and pCMV-EGFP-NMHC-IIAΔACD were described previously (27). All remaining MHC truncations were constructed using PCR methods, and all DNA segments subjected to PCR were sequenced to confirm the absence of PCR-generated errors. The plasmid pEGFP-C3-NMHC-IIA-ΔHead was constructed using a PCR product consisting of residue 775 through the EcoRI site at residue 1339, with an engineered 5′-HindIII site. This product was then ligated into pEGFP-C3-NMHC-IIA following removal of the HindIII-EcoRI segment. The plasmid p-EGFP-C3-NMHC-IIA-Rod was constructed in the same manner but begins with residue 1251. The remaining MHC truncations (GFP-IIA-T1, T-2, and T-3) were engineered with 5′-HindIII and 3′-KpnI restriction sites. These were ligated into pEGFP-C3-NMHC-IIA following digestion with HindIII and KpnI to remove the full-length MHC IIA.

Cell Culture and Transfection—HeLa (human cervical cancer) cells were purchased from Clontech and maintained in minimal essential medium (Invitrogen) supplemented to 10% fetal bovine serum, 1% L-glutamine, and 1% penicillin/streptomycin. COS-7 (African green monkey kidney fibroblast-like) cells were maintained in Dulbecco's modified Eagle's medium supplemented to 10% fetal bovine serum, 1% L-glutamine, and 1% penicillin/streptomycin. Cells were maintained at 37 °C, 5% CO_2. All transfections were carried out using the Lonza Group Amaxa Nucleofector system with the following conditions (solution, program): HeLa cells (R, I-13), COS-7 cells (R, W-01), and COS-7 cells during siRNA (V, A24).

Immunofluorescence—Cells were fixed in 1× PBS supplemented to 2 mM $MgCl_2$, 2 mM EGTA, and 4% formaldehyde. Cells were then permeabilized in 1× PBS containing 0.5% Triton X-100. Samples were blocked in 1× PBS with 3% fetal bovine serum and 0.1% Tween for 20 min. Primary and secondary antibody, phalloidin, and DAPI incubations were performed in blocking buffer for 1 h at room temperature. The following antibody/stain concentrations were used: NMHC-IIA 1:500 (Sigma, M8064), NMHC-IIB 1:500 (Sigma, M7939), Alexa Fluor-568 phalloidin (Molecular Probes) for staining of actin and 1 μg/ml DAPI for staining of DNA (Invitrogen). All images are single confocal sections taken on confocal microscopes with Plan-Apochromat 63×/1.4 NA oil objectives. Some images were acquired on a Zeiss LSM 510, and some were acquired on a Leica TCS-SP2.

Flow Cytometry to Assess Multinucleation—For immunohistochemistry and flow cytometry, siRNA was performed as follows. COS-7 cells were transfected with 200 pmol of MHC IIA or MHC IIB siRNA oligonucleotide (Dharmacon Smart Pool) and 5 μg of the indicated plasmid using the Lonza Group Amaxa Nucleofector system (solution V, program A24). These cells were plated and incubated at 37 °C for 72 h. Cells were collected using trypsin, and an equal number of cells for each transfection were successively pelleted and resuspended in medium containing 0.25% formaldehyde for 10 min at 37 °C, cold 90% methanol in 1× PBS for 20 min at −20 °C, 1× PBS for 1 min at 4 °C (2×), and 1× PBS containing 40 μg/ml RNase at 37 °C for 20 min and then 4 °C for 10 min. An equal volume of 1× PBS with propidium iodide was then added for a final propidium iodide concentration of 50 μg/ml, which was allowed to equilibrate for 1 h prior to analysis. Data were analyzed using ModFit.

Quantitation of Furrow Intensity—Z-series of early anaphase HeLa cells were acquired using a Leica TCS-SP2 with a Plan Apochromat 63×/1.4 NA oil objective. Images were collected with identical, subsaturating settings. Step size was set to 0.5 μm. The middle of the cell was defined as the slice with the largest pole to pole distance, and this slice was used for analysis. Line scans through the equatorial region were collected using the NIH ImageJ software. Line width was set to 15 pixels. Line "plot profiles" were exported from ImageJ. Data were analyzed and graphed as box plots using SigmaPlot.

RESULTS

RLC-independent Localization of Myosin to the Furrow—To determine whether RLC-phosphorylation-based *de novo* filament assembly in the furrow zone is the dominant mechanism of myosin localization to the equatorial region of dividing cells, we have used a GFP-tagged MHC IIA construct with a deleted RLC binding site (GFP-IIA-ΔIQ2; Fig. 1, *A* and *B*). This construct, previously shown to be incapable of binding RLC when expressed in HeLa cells, displays severe overassembly in live cells (27), and based on previous studies, is predicted to have

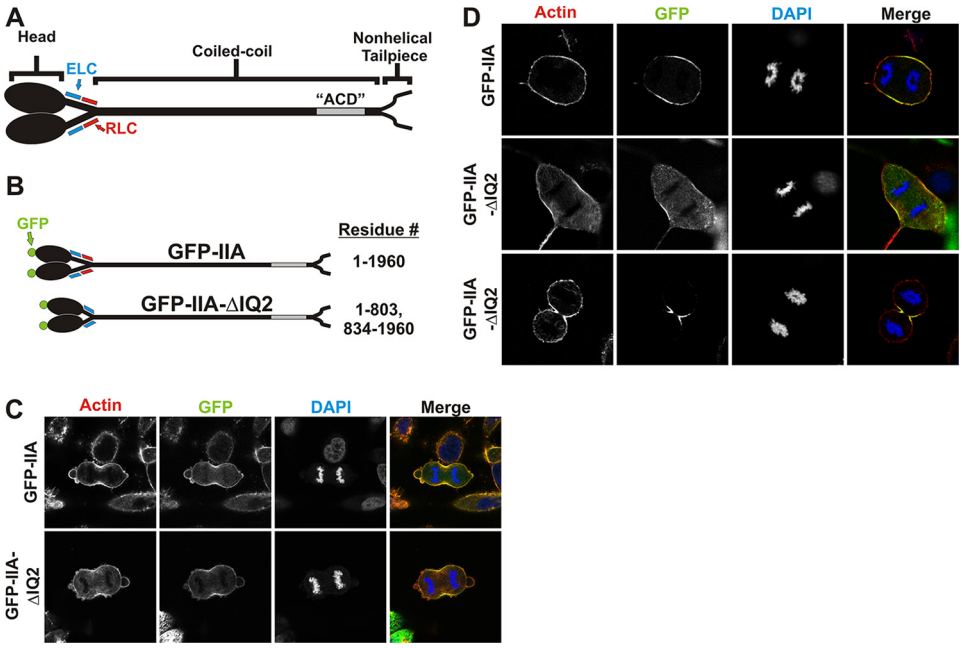

FIGURE 1. **RLC-independent localization of myosin to furrow in HeLa and COS-7 cells.** *A*, diagram of myosin IIA. GFP was conjugated to the amino terminus of the MHC. *B*, diagram of GFP-IIA constructs. GFP-IIA-ΔIQ2 removes the RLC binding site known as the IQ2 motif. *C* and *D*, at 72 h after transfection, HeLa (*C*) or COS-7 (*D*) cells expressing GFP-IIA (*top row*) or GFP-IIA-ΔIQ2 in early anaphase (*middle row*) or late anaphase (*lower row*) were fixed and stained with phalloidin-568 (*red*) for actin and DAPI (*blue*) for DNA. The images in the *right column* are merges of actin, DNA, and GFP channels.

constitutive motor activity (28). However, given that this myosin II construct has no associated RLC, the centralspindlin model that furrow-specific localized RLC phosphorylation drives contractile ring assembly would predict that this construct should not localize to the cytokinetic furrow.

Surprisingly, GFP-IIA-ΔIQ2 was able to localize to the furrow of dividing HeLa cells with similar robustness as GFP-tagged wild-type MHC IIA (GFP-IIA; Fig. 1*C*). Quantitative line scan analysis confirmed that GFP-IIA-ΔIQ2 is recruited to the furrow to a similar level as wild-type GFP-IIA (Fig. 2). This result suggests that in mammalian cells, myosin II furrow recruitment can occur independently of centralspindlin-based myosin II phosphorylation. However, the GFP-IIA-ΔIQ2 construct is likely capable of co-assembling into filaments with the endogenous MHC IIA that is present in HeLa cells, allowing the possibility that the endogenous MHC IIA is recruiting the GFP-IIA-ΔIQ2 into the furrow. To eliminate this possibility, we used COS-7 cells, which predominantly express MHC IIB with no detectable MHC IIA (supplemental Fig. S1) and only trace levels of MHC IIC expression (29). Similar to the results in HeLa cells, both wild-type GFP-IIA and GFP-IIA-ΔIQ2 were capable of localizing to the furrow in COS-7 (Fig. 1*D*). This is not an isoform-specific property as GFP-**IIB**-ΔIQ2 was able to localize to the furrow of dividing HeLa cells that express no endogenous MHC IIB (data not shown). This result demonstrates that localized activation of filament assembly, via furrow-restricted centralspindlin-driven RLC phosphorylation, is unnecessary for myosin II recruitment to the furrow.

GFP-IIA ΔIQ2 Localizes to the Furrow upon Depletion of Endogenous MHC IIB—Because it is unclear whether or not myosin II isoforms can co-assemble into heterotypic filaments (*i.e.* mixed filaments containing myosin IIA and myosin IIB), it remained a possibility that the myosin IIB present in COS-7 cells was responsible for the furrow localization of the GFP-IIA-ΔIQ2. To determine whether the GFP-IIA-ΔIQ2 was being recruited to the equatorial region via co-assembly with endogenous myosin IIB, we used siRNA to suppress MHC IIB expression in COS-7 cells, in conjunction with transfection of GFP-MHC-IIA-ΔIQ2. Upon depletion of MHC IIB (~87% knockdown; supplemental Fig. S2), GFP-IIA-ΔIQ2 is still able to localize to the equatorial region of dividing cells (Fig. 3*A*). These data argue that GFP-IIA-ΔIQ2 can be recruited to the furrow independently of any association with the endogenous MHC IIB.

GFP-IIA and GFP-IIA-ΔIQ2 Rescue Multinucleation upon MHC IIB siRNA—In agreement with previous reports (29), we found that knockdown of MHC IIB in COS-7 cells causes a multinucleation phenotype and that expression of GFP-IIA is able to rescue that phenotype (Fig. 3, *B* and *C*). To determine whether a myosin II lacking RLC could also rescue this multinucleation phenotype, we transfected MHC IIB siRNA together with the GFP-IIA-ΔIQ2 construct. GFP-positive cells were then analyzed for nucleation state using flow cytometry. Interestingly, GFP-IIA-ΔIQ2 was able to rescue the multinucleation phenotype nearly as well as wild-type GFP-IIA (Fig. 3*C*), indicating that this construct is not only recruited to the furrow but is also capable of driving efficient cell division.

Myosin IIA Can Bind to the Cortical Cytokinetic Furrow via Two Distinct Mechanisms—One possibility for the localization of GFP-IIA-ΔIQ2 in the absence of endogenous myosin is through an association with actin via its actin binding site, located in the amino-terminal globular motor or head domain. Recent studies in HeLa cells examined localization behavior of a truncated mammalian MHC IIA construct that lacked approximately one-half of the head domain (30). Although that construct clearly co-assembled with and disrupted stress fibers during interphase, during cell division, it formed dramatic punctate aggregates that did not localize to the furrow. To avoid possible aggregation effects and to assess whether the head is needed for furrow localization, we constructed GFP-MHC truncations that removed the entire head domain (GFP-IIA-ΔHead; this construct retains the ELC and RLC binding sites of the neck) or that removed both the entire head and the entire neck domains (GFP-IIA-Rod; Fig. 4*A*). Both of these constructs were capable of furrow localization in dividing COS-7 cells (Fig. 4*B*).

To determine whether the GFP-IIA-Rod could localize to the furrow independent of endogenous myosin, COS-7 cells were transfected with the GFP-IIA-Rod together with MHC IIB siRNA. These cells became noticeably multinucleate (Fig. 4*C*,

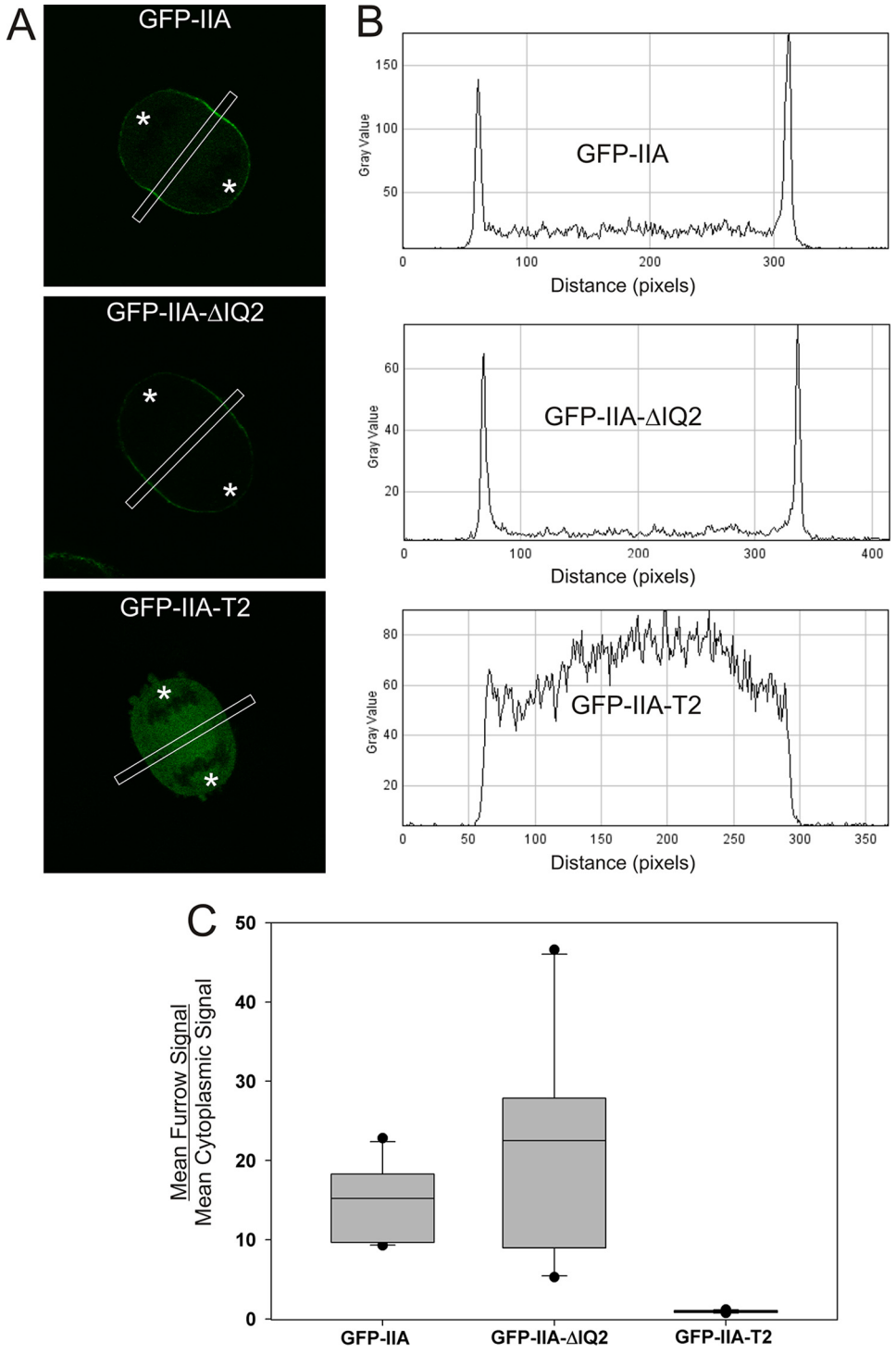

FIGURE 2. **GFP-IIA-ΔIQ2 localizes to furrow efficiently in HeLa cells.** *A*, HeLa cells were transfected with the indicated plasmid. Z-stacks of early anaphase cells were collected. The middle slice, defined as the slice with the largest pole-to-pole distance, was used for analysis. A 15-pixel-wide line was drawn through the equatorial region (shown as *white boxes* in *panel A*). *B*, the line scans were converted to plot profiles. *C*, for each furrow analyzed, the mean furrow signal and mean cytoplasmic signal were calculated. The box plot shows the ratio of furrow signal to cytoplasmic signal for 12 furrows per construct. The ends of the boxes define the 25th and 75th percentile, with a line at the median and error bars defining the 10th and 90th percentiles. *Dark circles* indicate the maximum and minimum. In *panel A*, *asterisks* indicate the approximate position of spindle poles.

lower panels). However, in these samples, GFP-IIA-Rod still localized reproducibly with actin in cortical regions between separated chromosomes of anaphase cells, where one would predict spindle-based contractile ring assembly signals to operate (Fig. 4*C*, *arrows*). However, this localization was not as dramatic or uniform as when endogenous myosin II is present (compare Fig. 4*B* and 4*C*), suggesting the possibility that some of the GFP-IIA-Rod recruitment in normal COS-7 furrows was mediated through heterotypic filament assembly with MHC IIB. These results demonstrate that the full-length myosin IIA tail binds to the cleavage furrow cortex even when endogenous myosin II is depleted.

To determine whether the multinucleation level induced upon expression of GFP-IIA-Rod with MHC IIB siRNA was similar to the multinucleation seen upon expression of GFP with MHC IIB siRNA or whether the GFP-IIA-Rod is capable of any rescue, we again used flow cytometry to analyze nucleation state. Expression of GFP-IIA-Rod did not rescue the multinucleation phenotype, and in fact, appeared to augment it (Fig. 3*C*). This supports previous reports using blebbistatin, a specific inhibitor of myosin II ATPase, showing that myosin II ATPase activity is necessary for cleavage furrow ingression and cytokinesis in HeLa cells (31).

To further map the tail domain(s) that mediate cortical furrow binding, we expressed a truncated tail fragment that extends from a region just upstream of the previously mapped *in vitro* assembly-competent domain (ACD) (32, 33) through the non-helical tailpiece (termed GFP-IIA-T1; Fig. 5*A*). As shown in Fig. 5*B*, GFP-IIA-T1 shows enrichment at the furrow, although its recruitment appears to be reduced when compared with the full-length rod. Further truncation of this region of the tail, from either the carboxyl-terminal or the amino-terminal ends (GFP-IIA-T2 and GFP-IIA-T3, respectively), completely abrogated enrichment at the equatorial region (Figs. 2 and 5, *A* and B). This behavior suggested that GFP-IIA-T1 might be localizing to the furrow via a co-assembly-based mechanism.

To determine whether GFP-IIA-T1 localization at the furrow was through co-assembly with the endogenous MHC IIB,

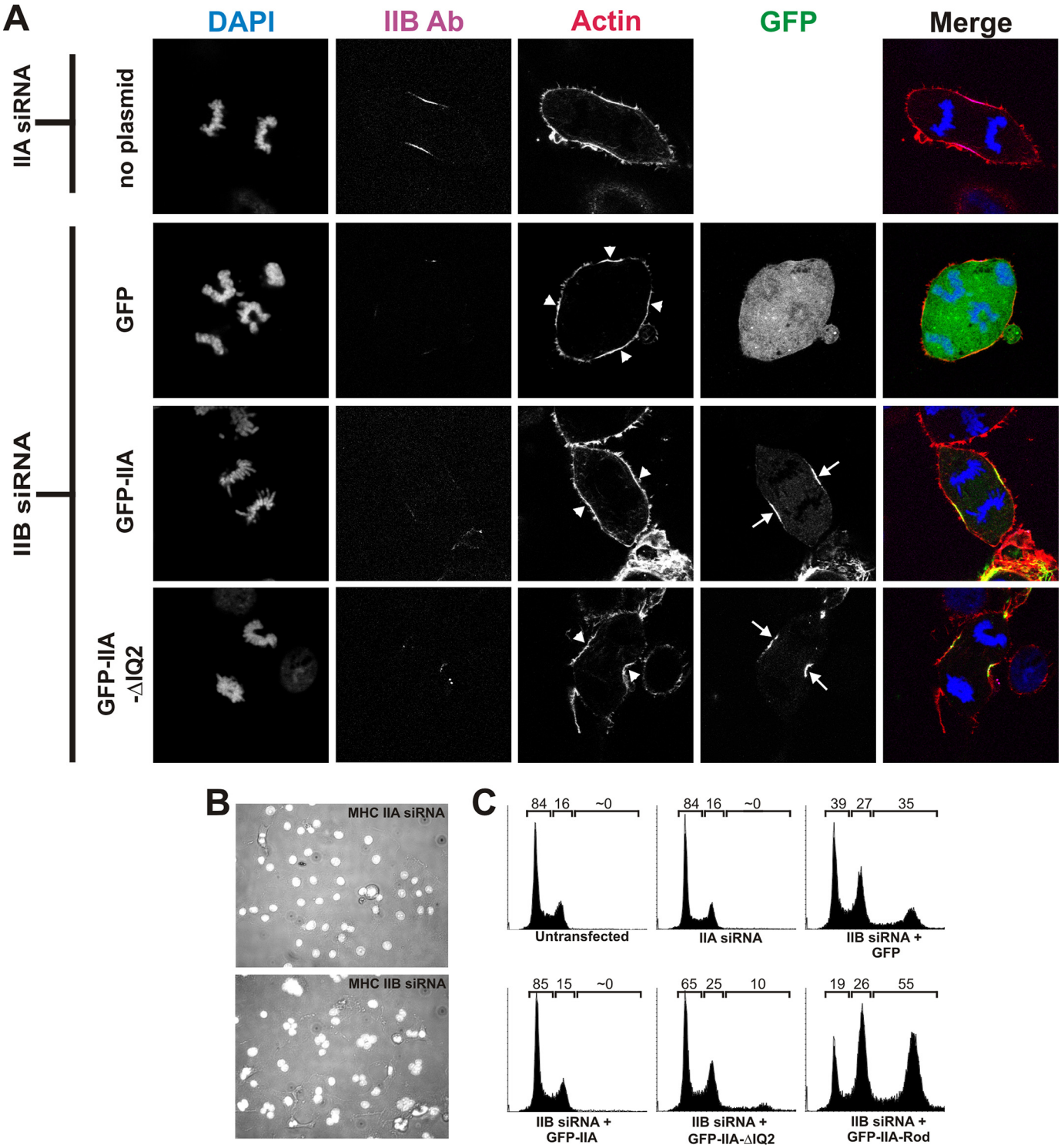

FIGURE 3. **GFP-IIA and GFP-IIA-ΔIQ2 localize to the furrow and rescue multinucleation in MHC IIB siRNA-treated COS-7 cells.** *A*, COS-7 cells were transfected with MHC IIA siRNA without plasmid (MHC IIA siRNA was used as a negative control; these cells do not express MHC IIA) or with MHC IIB siRNA together with plasmids expressing GFP, GFP-IIA, or GFP-IIA-ΔIQ. At 72 h after transfection, cells were fixed and stained for F-actin (*red*) and for DNA (*blue*) and immunostained for MHC IIB (*magenta*). MHC IIB images for each construct were collected using identical acquisition settings. The images in the *right column* are merges of actin, DNA, MHC IIB, and GFP channels. *Arrows* and *arrowheads* indicate the enrichment of GFP-IIA constructs and actin, respectively, in furrow zones. *Ab*, antibody. *B*, COS-7 cells were transfected with the MHC IIA (*top*) or MHC IIB (*bottom*) siRNA. The panels shown are merged images of bright field and DAPI (*white*) images acquired at 72 h. *C*, COS-7 cells were not transfected or were transfected with MHC IIA siRNA or with MHC IIB siRNA and the indicated plasmid. Cells were fixed 72 h after transfection, stained for DNA content using propidium iodide, and analyzed using flow cytometry. The *numbers* above each graph represent the percentage of the total population possessing a DNA content of less than 4*n* (*left number*), 4*n* (*center number*), or greater than 4*n* (*right number*).

we again used siRNA to deplete MHC IIB while simultaneously expressing GFP-IIA-T1. Upon siRNA of MHC IIB, we were unable to find any cells in anaphase with GFP-IIA-T1 localization or enrichment in the equatorial region (Fig. 5*C*, *lower panels*), supporting the model that GFP-IIA-T1 recruitment is mediated through a co-assembly with the endogenous MHC

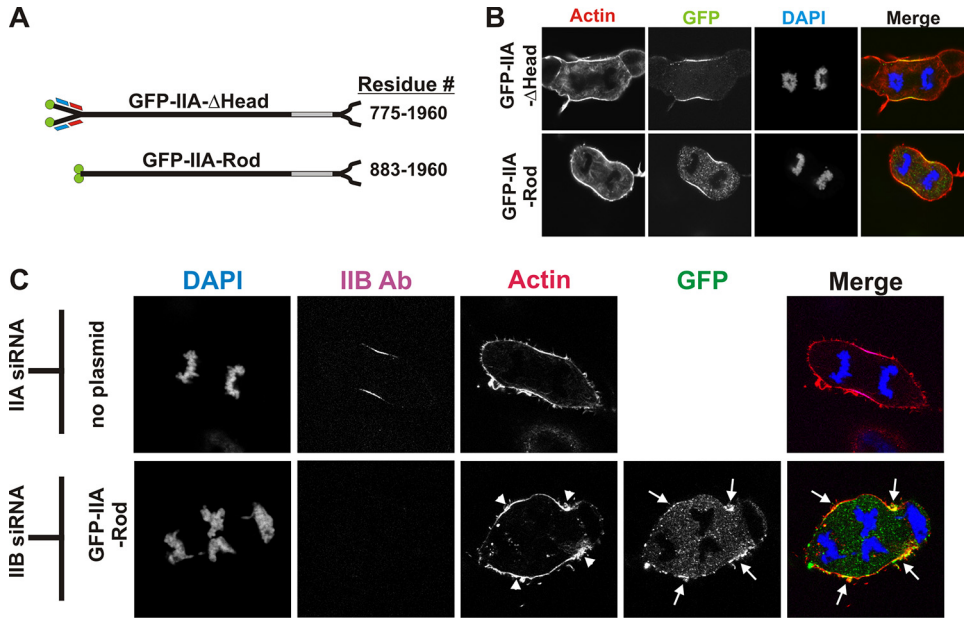

FIGURE 4. **Headless myosin IIA can localize to the furrow in COS-7.** *A*, diagram of GFP-IIA-ΔHead and GFP-IIA-Rod constructs with their corresponding residues. *B* and *C*, at 72 h after transfection, COS-7 cells expressing GFP-IIA-ΔHead, or GFP-IIA-Rod or COS-7 cells transfected with MHC IIA siRNA or with MHC IIB siRNA together with GFP-IIA-Rod were fixed and stained for F-actin (*red*) and for DNA (*blue*). The samples in *panel C* were also immunostained for MHC IIB to identify cells that received the siRNA. The images in the *right column* are merges of all other channels in the panel. *Arrows* and *arrowheads* indicate the enrichment of GFP-IIA-Rod and actin, respectively, in furrow zones.

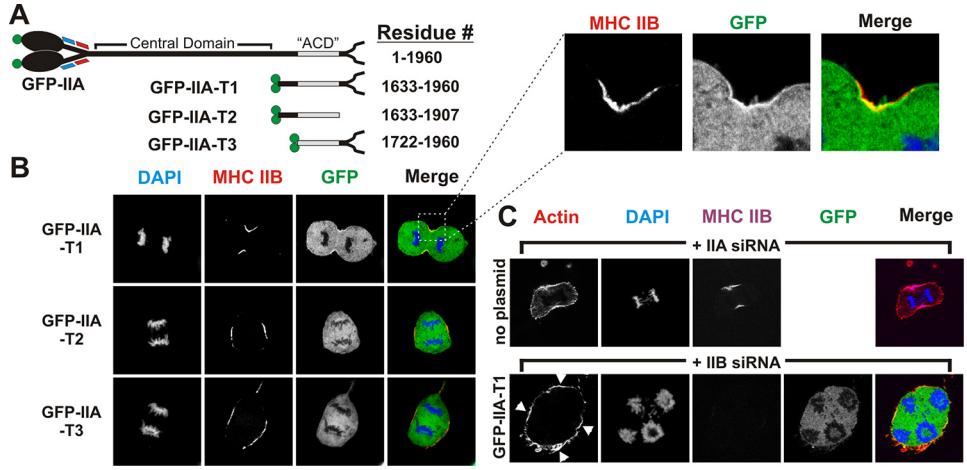

FIGURE 5. **The carboxyl terminus of MHC IIA can localize to the furrow in an MHC IIB-dependent manner.** *A*, diagram of GFP-MHC-IIA truncation constructs and their corresponding residues. The ACD is shown in *gray*. *B*, COS-7 cells were transfected with GFP-IIA-T1, -T2, or -T3. At 72 h after transfection, cells were fixed and stained for DNA (*blue*) and immunostained for MHC IIB (*red*). *C*, COS-7 cells were transfected with MHC IIA siRNA or with MHC IIB siRNA and plasmid encoding construct GFP-IIA-T1. At 72 h after transfection, cells were fixed and stained for F-actin (*red*) and for DNA (*blue*) and immunostained for MHC IIB (*magenta*). *Arrowheads* indicate the enrichment of actin in furrow zones.

IIB. Thus sequences in and adjacent to the ACD of myosin IIA can drive co-assembly with endogenous myosin IIB in the furrow (Fig. 5), but additional sequences in the central domain of myosin IIA can drive localization to the furrow cortex even in the absence of endogenous myosin IIA or IIB (Fig. 4).

DISCUSSION

Multiple recent studies have revealed a conserved signaling pathway involving the centralspindlin complex (MKLP1, MgcRacGAP, ECT2) that activates effectors involved in contractile ring assembly (34, 35). Recent work from Oegema and colleagues (36) has shown the *Caenorhabditis elegans* homolog of MgcRacGAP, CYK-4, to have additional roles besides the previously known function of anchoring ECT2 to MKLP1. CYK-4 was shown to be critical for the inactivation of Rac in the central spindle to prevent activation of the Arp2/3 complex, which could theoretically lead to disarrayed actin cytoskeleton in the contractile ring (36). Another downstream effector of the centralspindlin complex is RhoA, which is activated through the GEF activity of ECT2 (37). RhoA is known to activate the formin mDia2, leading to nucleation of parallel actin filaments at the furrow (34, 38). It has been proposed that the centralspindlin complex acts synergistically with anillin to stabilize RhoA at the cleavage furrow (25). In this model, both RhoA-containing complexes then facilitate localized activation of Rho kinase and citron kinase, leading to localized phosphorylation of the RLC to promote myosin II activation and assembly (14, 15, 18). The studies presented here demonstrate that robust myosin II recruitment to the furrow can be achieved without spatially localized centralspindlin-mediated RLC phosphorylation. Clearly other recruitment pathways such as cortical flow (22, 24) and/or equatorial myosin II binding partners (25, 26) are sufficient for myosin II recruitment and cell furrowing in mammalian cells. Our data argue that in mammalian cells, the centralspindlin complex may be critical for activating these other recruitment pathways and that, in fact, this alternative role for centralspindlin may be more important than any possible role in driving localized RLC phosphorylation. It is important to note that many of these conclusions are derived from work with a constitutively active myosin II (GFP-IIA-ΔIQ2). Without direct disruption of the centralspindlin complex, we cannot rule out its involvement in furrow recruitment of normal myosin II, whether it is through RLC-dependent or -independent mechanisms.

Based on previous work in *Dictyostelium* (28), we hypothesized that the GFP-IIA-ΔIQ2 construct would be constitutively active. Our rescue data support this hypothesis (Fig. 3*C*), although the rescue does not appear to be complete. This dif-

ference in rescue between full-length GFP-IIA and GFP-IIA-ΔIQ2 does not appear to be due to a difference in expression as both express at similar levels (data not shown). One possibility is that removal of the IQ2 region from mammalian myosin II does not result in the same level of constitutive activity as was previously shown in *Dictyostelium*. Another possibility is that IQ2 removal eliminates RLC phosphorylation and dephosphorylation, thereby drastically decreasing myosin assembly turnover in the contractile ring. Previous studies in *Dictyostelium* have shown that constitutive myosin II overassembly can lead to an elevated failure rate in completion of cytokinesis (39). Further studies will be required to elucidate these possibilities.

This is the first report in mammalian cells of headless myosin localizing to the furrow independent of endogenous myosin II. This observation is intriguing and consistent with previous reports demonstrating rod localization to the furrow in lower eukaryotes such as *Dictyostelium* and fission yeast (40, 41). Previous reports have suggested that actin is required for myosin II association with the cortex (21) and that myosin II is required for the cortical flow of actin (23). Therefore, because these rod constructs are presumed not to bind actin, it is unlikely that they are localizing via cortical flow. Myosin IIA rod recruitment requires the presence of the amino-terminal region of the rod (compare GFP-IIA-Rod (Fig. 4*C*) with GFP-IIA-T1 (Fig. 5*C*)), suggesting that cortical furrow proteins bind this central domain of MHC IIA to facilitate recruitment to the furrow. Two interesting candidates that may mediate this binding are septins (26) and anillin, which is known to stabilize myosin in the contractile ring (25).

Finally, we show that the carboxyl-terminal region of MHC IIA that contains the ACD is able to localize to the furrow in the presence of MHC IIB but not when MHC IIB expression is suppressed using siRNA. This result promotes two interesting observations. The first is the possibility of a positive feedback mechanism for myosin localization to the furrow in which equatorial myosin II filaments can further recruit myosin molecules in an ACD-dependent manner. The second is that myosin IIA and IIB are capable of co-assembling into heterotypic filaments during cell division. In summary, the behavior of our myosin IIA truncations reveals two distinct modes by which the myosin IIA tail can bind to the furrow cortex. Constructs containing the central domain bind the furrow cortex independent of endogenous myosin IIA or IIB, and the myosin IIA ACD can bind through a mechanism requiring the presence of the IIB isoform, indicating heterotypic filament assembly. We suggest that these independent anchoring mechanisms operate synergistically to facilitate myosin II filament accumulation in the furrow.

Acknowledgments—We thank Robert Adelstein and Xufei Ma for technical advice.

REFERENCES

1. Totsukawa, G., Himi-Nakamura, E., Komatsu, S., Iwata, K., Tezuka, A., Sakai, H., Yazaki, K., and Hosoya, H. (1996) *Cell Struct. Funct.* **21,** 475–482
2. Yamakita, Y., Yamashiro, S., and Matsumura, F. (1994) *J. Cell Biol.* **124,** 129–137
3. Conti, M. A., Sellers, J. R., Adelstein, R. S., and Elzinga, M. (1991) *Biochemistry* **30,** 966–970
4. Murakami, N., Chauhan, V. P., and Elzinga, M. (1998) *Biochemistry* **37,** 1989–2003
5. Sellers, J. R., Spudich, J. A., and Sheetz, M. P. (1985) *J. Cell Biol.* **101,** 1897–1902
6. Sellers, J. R., Pato, M. D., and Adelstein, R. S. (1981) *J. Biol. Chem.* **256,** 13137–13142
7. Craig, R., Smith, R., and Kendrick-Jones, J. (1983) *Nature* **302,** 436–439
8. Golomb, E., Ma, X., Jana, S. S., Preston, Y. A., Kawamoto, S., Shoham, N. G., Goldin, E., Conti, M. A., Sellers, J. R., and Adelstein, R. S. (2004) *J. Biol. Chem.* **279,** 2800–2808
9. Bao, J., Ma, X., Liu, C., and Adelstein, R. S. (2007) *J. Biol. Chem.* **282,** 22102–22111
10. Murakami, N., Kotula, L., and Hwang, Y. W. (2000) *Biochemistry* **39,** 11441–11451
11. Marini, M., Bruschi, M., Pecci, A., Romagnoli, R., Musante, L., Candiano, G., Ghiggeri, G. M., Balduini, C., Seri, M., and Ravazzolo, R. (2006) *Int. J. Mol. Med.* **17,** 729–736
12. Kolega, J. (1998) *J. Cell Sci.* **111,** 2085–2095
13. Kelley, C. A., Sellers, J. R., Gard, D. L., Bui, D., Adelstein, R. S., and Baines, I. C. (1996) *J. Cell Biol.* **134,** 675–687
14. Kamijo, K., Ohara, N., Abe, M., Uchimura, T., Hosoya, H., Lee, J. S., and Miki, T. (2006) *Mol. Biol. Cell* **17,** 43–55
15. Eda, M., Yonemura, S., Kato, T., Watanabe, N., Ishizaki, T., Madaule, P., and Narumiya, S. (2001) *J. Cell Sci.* **114,** 3273–3284
16. Madaule, P., Furuyashiki, T., Eda, M., Bito, H., Ishizaki, T., and Narumiya, S. (2000) *Microsc. Res. Tech.* **49,** 123–126
17. Yamashiro, S., Totsukawa, G., Yamakita, Y., Sasaki, Y., Madaule, P., Ishizaki, T., Narumiya, S., and Matsumura, F. (2003) *Mol. Biol. Cell* **14,** 1745–1756
18. Dean, S. O., and Spudich, J. A. (2006) *PLoS. ONE.* **1,** e131
19. Miyauchi, K., Yamamoto, Y., Kosaka, T., and Hosoya, H. (2006) *Biochem. Biophys. Res. Commun.* **350,** 543–548
20. Mandato, C. A., Benink, H. A., and Bement, W. M. (2000) *Cell Motil. Cytoskeleton* **45,** 87–92
21. Yumura, S., Ueda, M., Sako, Y., Kitanishi-Yumura, T., and Yanagida, T. (2008) *Traffic* **9,** 2089–2099
22. DeBiasio, R. L., LaRocca, G. M., Post, P. L., and Taylor, D. L. (1996) *Mol. Biol. Cell* **7,** 1259–1282
23. Zhou, M., and Wang, Y. L. (2008) *Mol. Biol. Cell* **19,** 318–326
24. Yumura, S. (2001) *J. Cell Biol.* **154,** 137–146
25. Piekny, A. J., and Glotzer, M. (2008) *Curr. Biol.* **18,** 30–36
26. Joo, E., Surka, M. C., and Trimble, W. S. (2007) *Dev. Cell* **13,** 677–690
27. Breckenridge, M. T., Dulyaninova, N. G., and Egelhoff, T. T. (2009) *Mol. Biol. Cell* **20,** 338–347
28. Uyeda, T. Q., and Spudich, J. A. (1993) *Science* **262,** 1867–1870
29. Bao, J., Jana, S. S., and Adelstein, R. S. (2005) *J. Biol. Chem.* **280,** 19594–19599
30. Wei, Q., and Adelstein, R. S. (2000) *Mol. Biol. Cell* **11,** 3617–3627
31. Straight, A. F., Cheung, A., Limouze, J., Chen, I., Westwood, N. J., Sellers, J. R., and Mitchison, T. J. (2003) *Science* **299,** 1743–1747
32. Sato, M. K., Takahashi, M., and Yazawa, M. (2007) *Mol. Biol. Cell* **18,** 1009–1017
33. Nakasawa, T., Takahashi, M., Matsuzawa, F., Aikawa, S., Togashi, Y., Saitoh, T., Yamagishi, A., and Yazawa, M. (2005) *Biochemistry* **44,** 174–183
34. Barr, F. A., and Gruneberg, U. (2007) *Cell* **131,** 847–860
35. Werner, M., and Glotzer, M. (2008) *Biochem. Soc. Trans.* **36,** 371–377
36. Canman, J. C., Lewellyn, L., Laband, K., Smerdon, S. J., Desai, A., Bowerman, B., and Oegema, K. (2008) *Science* **322,** 1543–1546
37. Yüce, O., Piekny, A., and Glotzer, M. (2005) *J. Cell Biol.* **170,** 571–582
38. Watanabe, S., Ando, Y., Yasuda, S., Hosoya, H., Watanabe, N., Ishizaki, T., and Narumiya, S. (2008) *Mol. Biol. Cell* **19,** 2328–2338
39. Yumura, S., Yoshida, M., Betapudi, V., Licate, L. S., Iwadate, Y., Nagasaki, A., Uyeda, T. Q., and Egelhoff, T. T. (2005) *Mol. Biol. Cell* **16,** 4256–4266
40. Wong, K. C., D'souza, V. M., Naqvi, N. I., Motegi, F., Mabuchi, I., and Balasubramanian, M. K. (2002) *Curr. Biol.* **12,** 724–729
41. Zang, J. H., and Spudich, J. A. (1998) *Proc. Natl. Acad. Sci. U.S.A.* **95,** 13652–13657